

Solar Cells, Modules, Arrays, and Characterization

April 17, 2014

The University of Toledo, Department of Physics and Astronomy
SSARE, PVIC

Principles and Varieties of Solar Energy (PHYS 4400)



Topics

Solar Cells – current and voltage

Wiring up a c-Si solar module – typical current and voltage

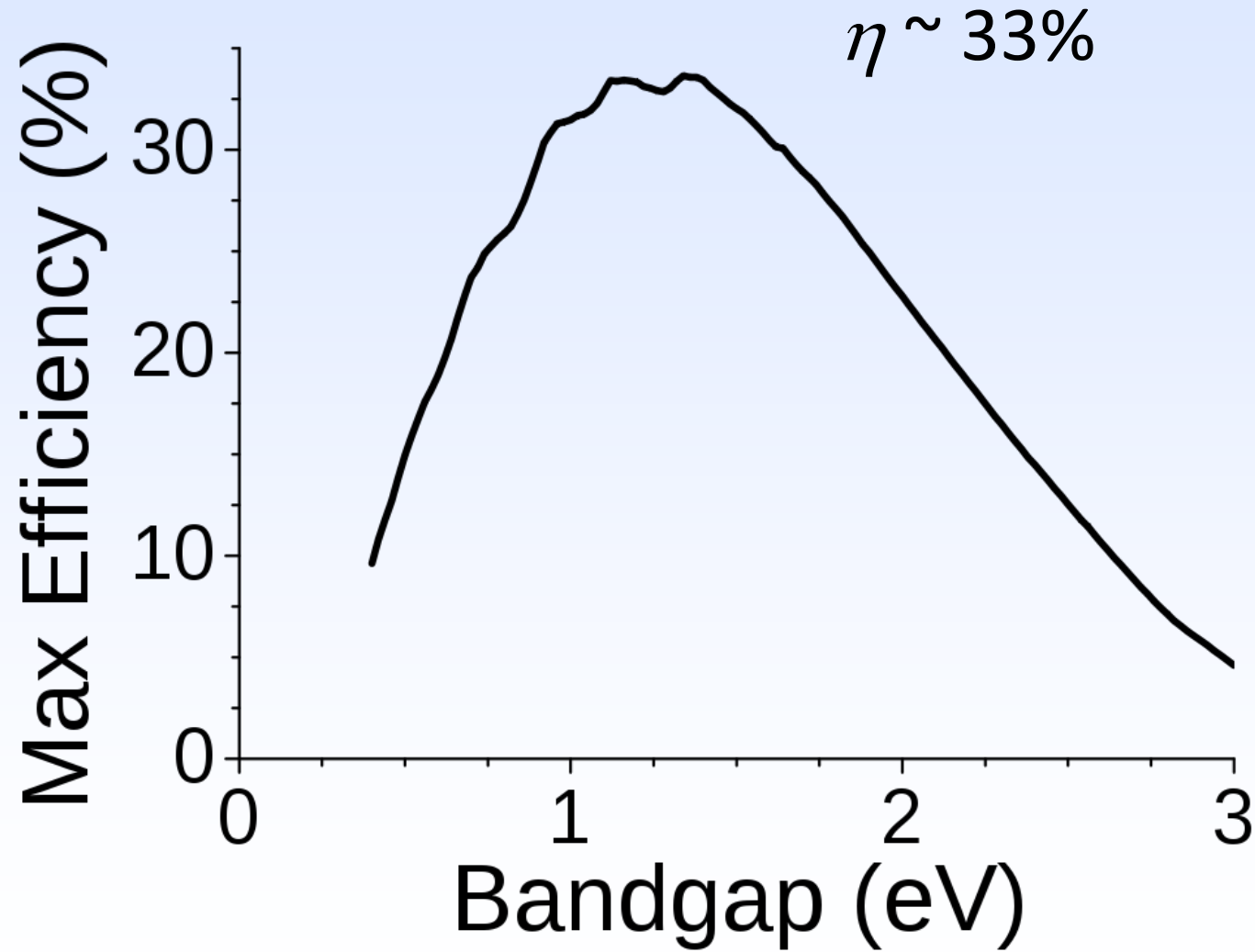
Wiring up a CdTe module

An example of a PV Array – 6 kW system

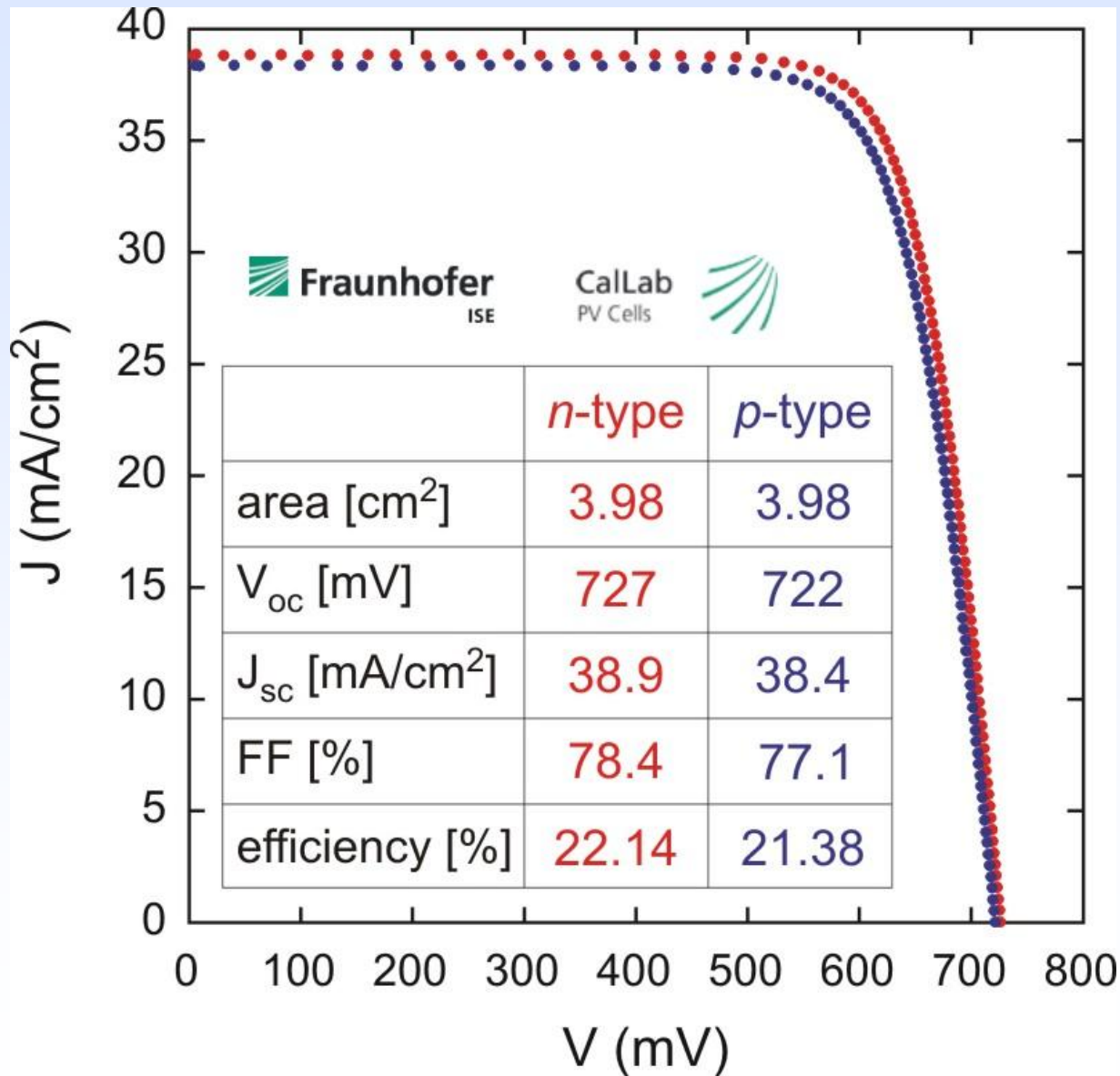
Techniques for characterizing photovoltaic materials, cells, and modules



Getting everything right...



monocrystalline Si solar cell



Isofoton ISF-250 monocrystalline Si module

ELECTRICAL CHARACTERISTICS

Performance at STC: Irradiance, 1.000 W/m²; cell temperature, 25° C (77° F); AM, 1.5

	ISF - 245	ISF - 250
Rated Power (Pmax)	245 W	250 W
Open Circuit Voltage (Voc)	37,6 V	37,8 V
Short-circuit Current (Isc)	8,63 A	8,75 A
Maximum power point Voltage (Vmax)	30,5 V	30,6 V
Maximum power point Current (Imax)	8,04 A	8,17 A
Efficiency	14,8 %	15,1 %
Power tolerance (% Pmax)	0/+3 %	0/+3 %

Performance at Irradiance 800 W/m², NOCT, ambient temperature 20° C (68° F), AM 1.5; wind speed 1 m/s

	ISF - 245	ISF - 250
Maximum Power (Pmax)	178 W	181 W
Open Circuit Voltage (Voc)	34,8 V	35,0 V
Short-circuit Current (Isc)	6,96 A	7,06 A
Maximum power point Voltage (Vmax)	27,4 V	27,5 V
Maximum power point Current (Imax)	6,49 A	6,59 A

Efficiency reduction from 1.000 W/m² to 200 W/m² according to standard IEC 60904-1 5% (+/-3%)

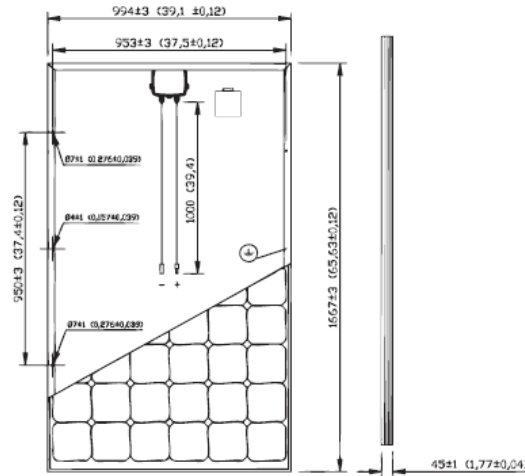
OPERATIONAL CHARACTERISTICS

Maximum System Voltage	600 V (UL) / 1000 V (IEC)
Series Fuse Rating	20 A
Nominal Operating Cell Temperature (NOCT)	47 +/- 2°C (116.6 +/- 3.5 F)
Operating Temperature	-40 to +85°C (-40 to 185 F)
Temperature Coefficient of Pmax	-0,44%/K
Temperature Coefficient of Voc	-0,334%/K
Temperature Coefficient of Isc	0,048%/K

MECHANICAL CHARACTERISTICS

Solar Cell	Monocrystalline Silicon - 156 mm x 156 mm (6 inches)
Number of cells	60 cells (6x10)
Dimensions	1667 x 994 x 45 mm (65.63 x 39.13 x 1.77 in)
Weight	19 kg (41.89 pounds)
Glass	High transmittance, patterned, tempered, 3,2 mm (EN-12150)
Frame	Anodized aluminum, grounding drills
Maximum mechanical load	5400 Pa (112.78 psf) (Snow load)
Junction Box	IP 65 with 3 bypass diodes
Cables, plug	Solar cable 1 m (39.37 in), 4 mm ² (12 AWG). MC4 or LC4

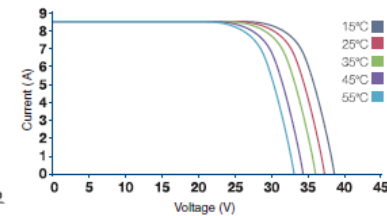
DIMENSIONS



PACKAGING

Modules per pallet
24

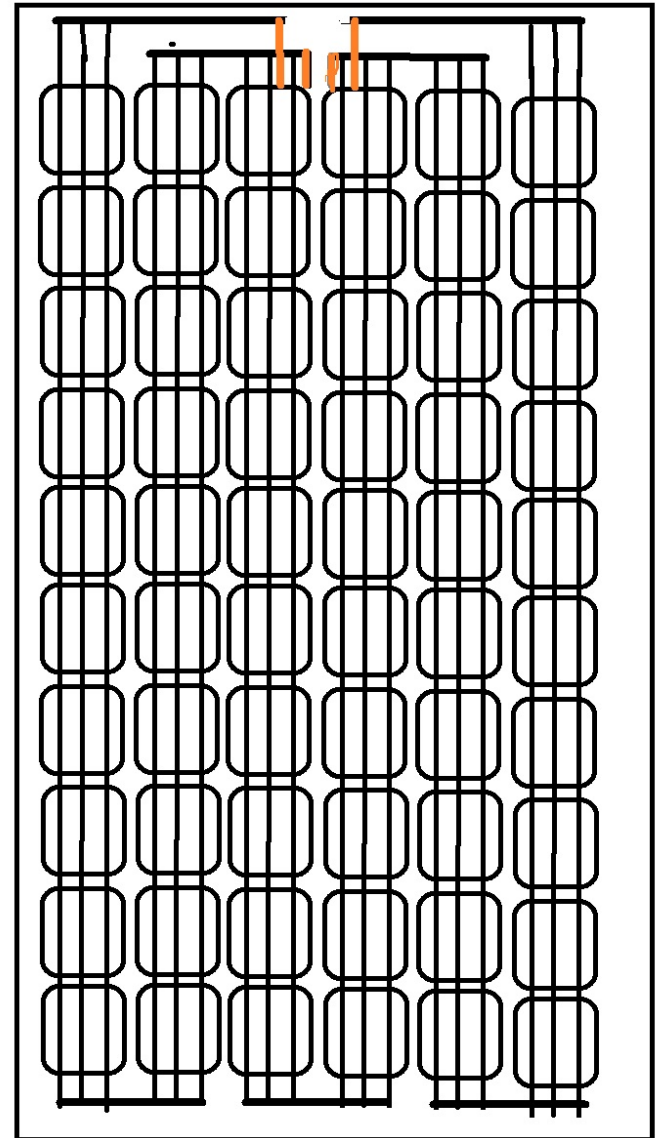
Packaging size (pallet+carton)
1720 x 1140 x 1155 mm
(5.64 x 3.74 x 3.79 feet)
Recyclable materials



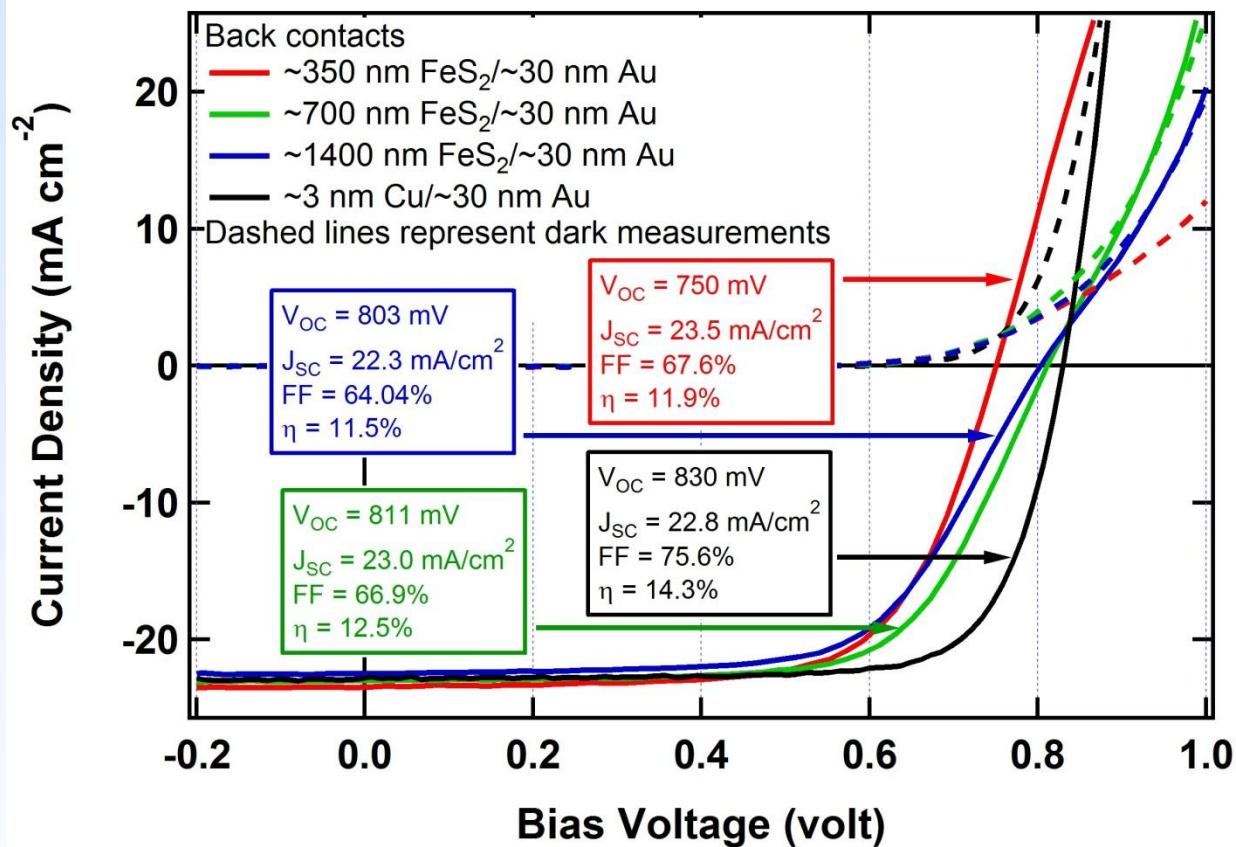
Isofoton ISF-250 monocrystalline Si module

At STC, and at mpp:

- 60 cells, wired in series $\rightarrow 60 \times 0.51 \text{ V} = 30.6 \text{ V}$
- Total current = $8.17 \text{ A} / 220 \text{ cm}^2 = 37.1 \text{ mA/cm}^2$
current density at mpp
- **Module efficiency** = Power Output / Power Incident
 $= 250 \text{ W} / [(1000 \text{ W} / (100 \text{ cm}^2)) (160 \times 100 \text{ cm}^2)] = 15.6\%$
- Cell efficiency is higher (~18-19%).
- Orange leads connect to J-Box (contains bypass diodes to prevent bad module taking down the array)



CdTe Solar Cell



At STC, and at mpp:

- For record device, J_{SC} is higher, 28 mA cm^{-2}
- V_{OC} also higher, 0.880 V
- With FF = 0.77, $\eta \cong 19\%$

Photoluminescence Lifetime System Specifications

Free Space Beam Height:

AOTF: 26 mm (may need a periscope)

iHR320: 98mm (from bottom of instrument)

Temporal Pulse Width of the Fianium: ~5 ps

Excitation Wavelength Range:

<420 nm to >2 μm from the light source, and 400 nm-1100 nm from the Frequency Tuner.

Detection Wavelength Range:

Hamamatsu H10330A-45 NIR PMT: 950 - 1400 nm

Hamamatsu R10467U-50 Hybrid PD: 380 - 890 nm

Transit Time Spread:

H10330A-45 NIR PMT: 400 ps,

Rise/Fall: 900 ps/1.7 ns,

R10467U-50 Hybrid PD: 90 ps,

Rise/Fall: 400/400 ps, Width: 600 ps

Pulse Repetition Rate: 20 MHz, 10 MHz, 5 MHz, 2 MHz, and 1 MHz

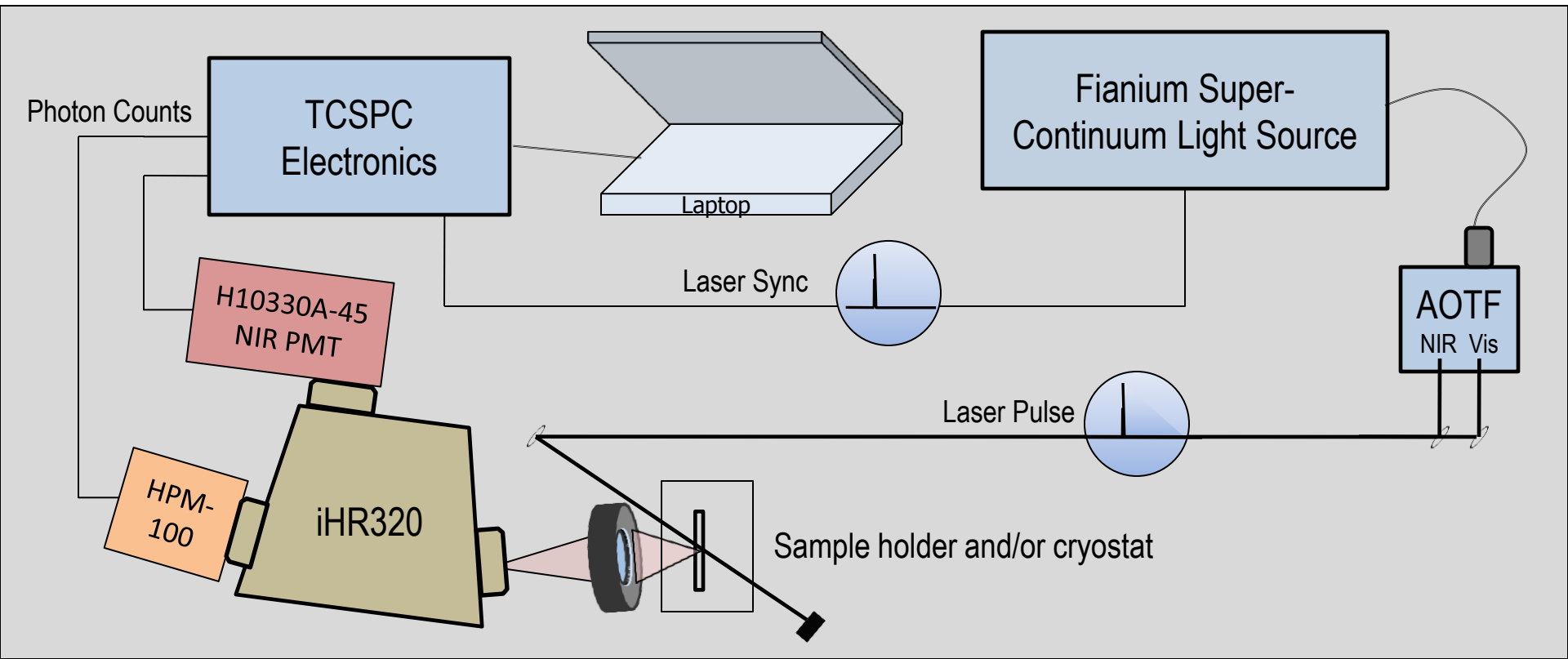
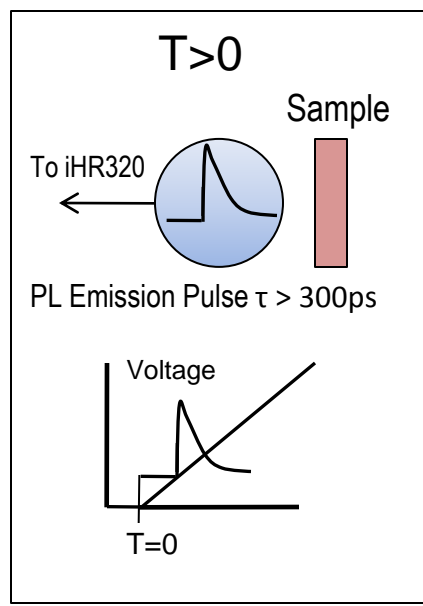
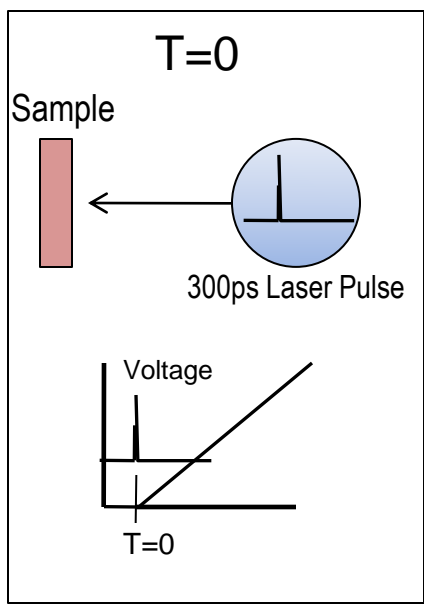
Pulse Energy: ~0.25 nJ/(5 nm Channel) @ 20 MHz, or 2 nJ with all 8 channels.

Time Correlated Single Photon Counting

$T=0$: The sync from the laser is registered in the Time to Amplitude Converter.

$T>0$: Photons emitted from the sample reach the detector and are counted. Their count time is found from the voltage of the count.

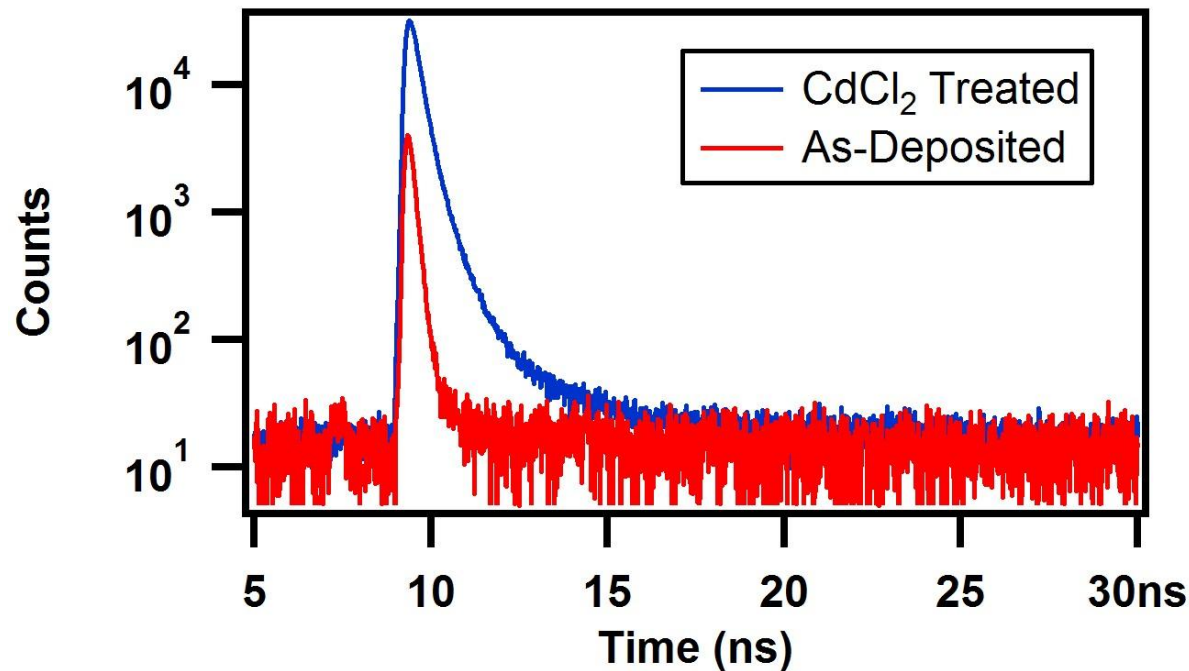
$T \gg 0$: This is repeated millions of times per second and a histogram depicts the photons collected as a function of time from the sync.



Sample PL Lifetime Data

CdTe solar cells are understood to benefit from crystal quality correlated with increased minority carrier lifetime. The minority carrier lifetime can be measured using time-resolved PL, since the PL intensity depends on the product of the free electron and free hole concentrations:

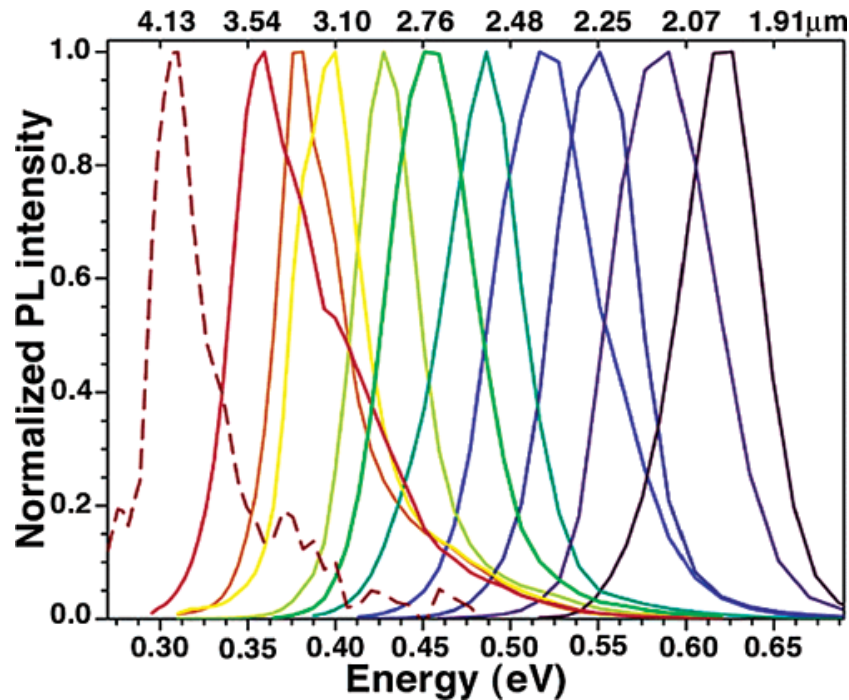
$$I_{PL}(t, E) \propto n(E, t) p(E, t)$$



TRPL measurements from untreated (as-deposited) CdTe are a good test of a PL lifetime system's sensitivity because emission intensity is quite low at room temperature. The above graph shows the PL lifetime data for treated vs. untreated CdTe at a fixed excitation pulse energy. The activated CdTe film shows an increase in the peak PL intensity of ~10x, and an increase in the lifetime by ~10x. Together these factors yield a strong increase in the time-integrated PL intensity (not shown).

Measuring bandgap (PL)

Photoluminescence (occurs at the bandgap for direct gap semiconductors)



Pushing the Band Gap Envelope: Mid-Infrared Emitting Colloidal PbSe Quantum Dots, J. AM. CHEM. SOC. 2004, 126, 11752-11753, Hollingsworth et al.

Bandgap can also be measured with:

- SPS – surface photovoltage spectroscopy
- Spectroscopic ellipsometry (?)



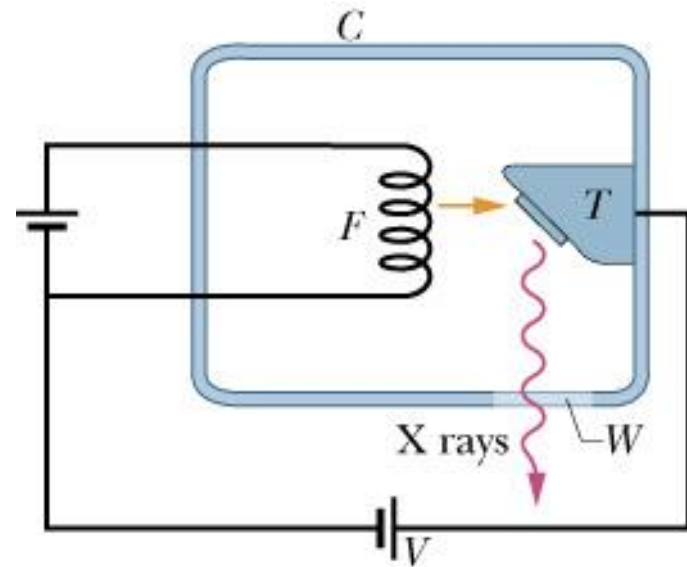
X-Ray Diffraction

Structural properties

X-Ray Generation

X-rays are electromagnetic radiation with wavelength $\sim 1 \text{ \AA} = 10^{-10} \text{ m}$ (visible light $\sim 5.5 \times 10^{-7} \text{ m}$)

X-ray generation: electrons are emitted from the cathode and accelerated toward the anode. Here, Bremsstrahlung radiation occurs as a result of the “braking” process – X-ray photons are emitted.



X-ray wavelengths too short to be resolved by a standard optical grating

$$\theta = \sin^{-1} \frac{m\lambda}{d} = \sin^{-1} \frac{(1)(0.1 \text{ nm})}{3000 \text{ nm}} = 0.0019^\circ$$

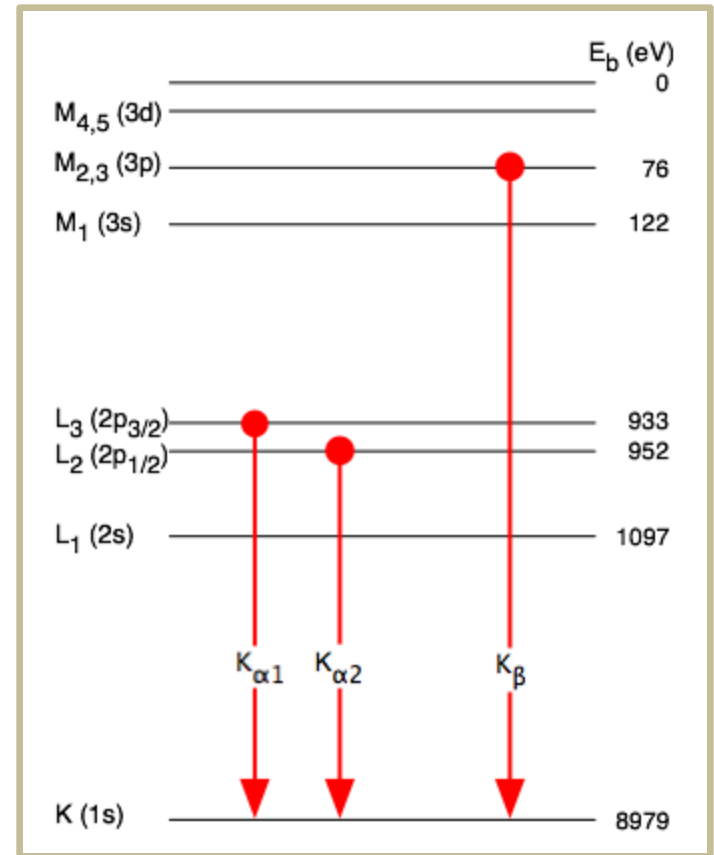
X-Ray Generation

The most common metal used is copper, which can be kept cool easily, due to its high thermal conductivity, and which produces strong K_α and K_β lines. The K_β line is sometimes suppressed with a thin ($\sim 10\ \mu\text{m}$) nickel foil.

- **K-alpha (K_α)** emission lines result when an electron transitions to the innermost "K" shell (principal quantum number 1) from a 2p orbital of the second or "L" shell (with principal quantum number 2).
- The K_α line is actually a doublet, with slightly different energies depending on spin-orbit interaction energy between the electron spin and the orbital momentum of the 2p orbital.

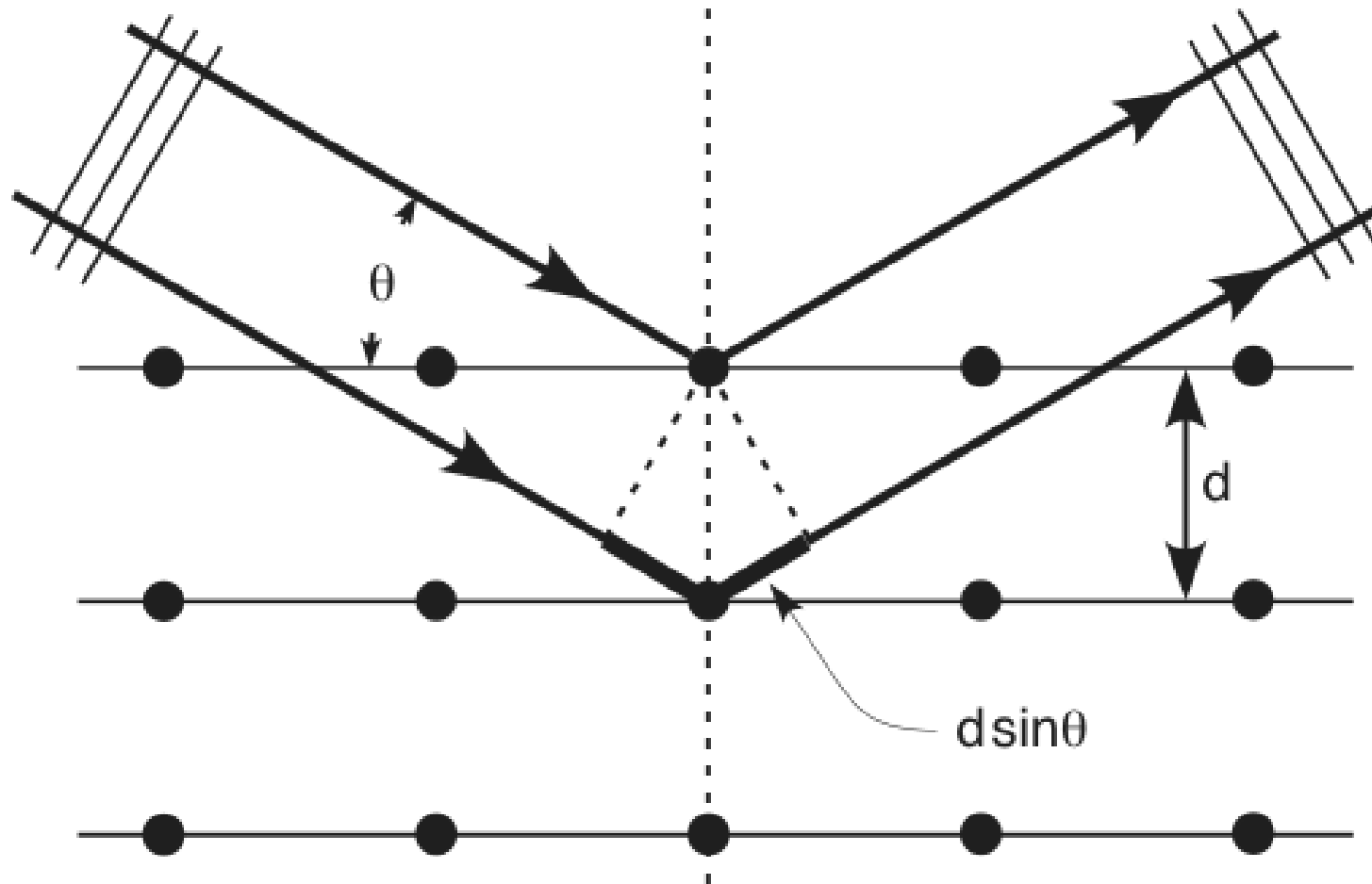
$$\lambda(K_\alpha) = 0.154\ \text{nm}$$

$$\lambda(K_\beta) = 0.139\ \text{nm}$$

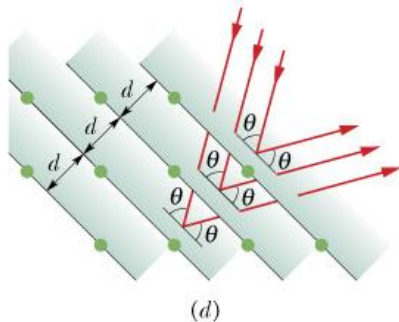
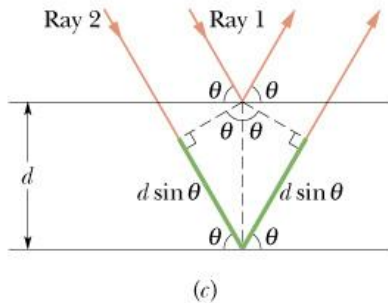
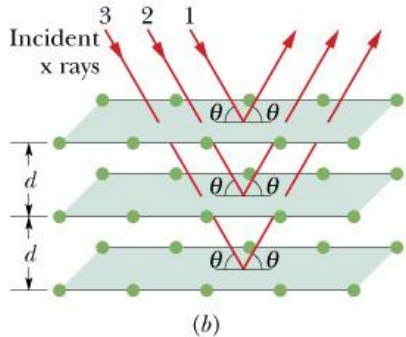
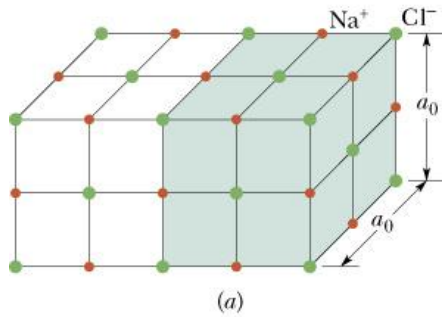


Atomic levels involved in copper K_α and K_β emission.

X-Ray diffraction



X-Ray Diffraction -- Bragg's Law



Diffraction of x-rays by crystal: spacing d of adjacent crystal planes on the order of 0.1 nm

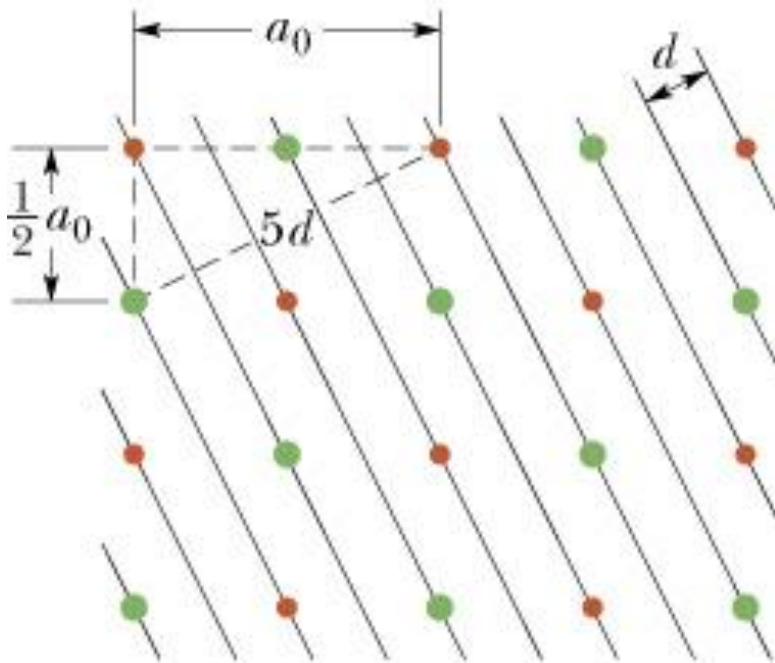
→ three-dimensional diffraction grating with diffraction maxima along angles where reflections from different planes interfere constructively

$$2d \sin \theta = m\lambda \text{ for } m = 0, 1, 2, \dots$$

Bragg's Law

Note that your measured XRD spectra will most likely reveal only 1st order diffracted lines (i.e., those for which $m = 1$).

X-Ray Diffraction, cont'd

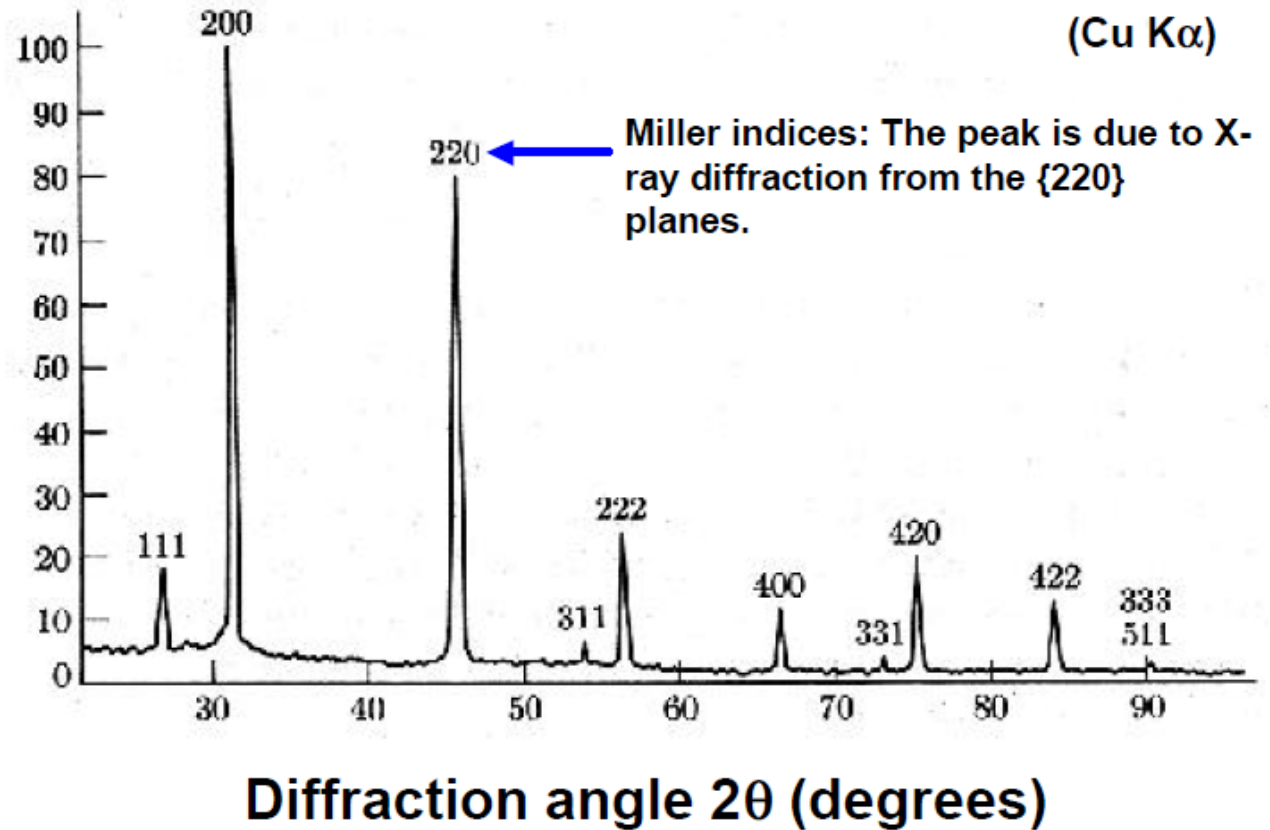
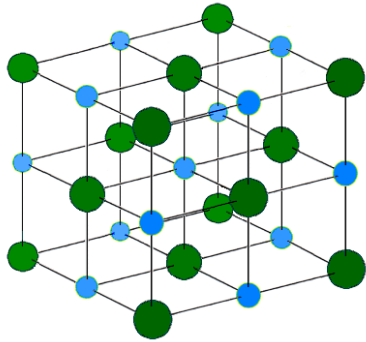


Interplanar spacing d is related to the unit cell dimension a_0

$$5d = \sqrt{\frac{5}{4} a_0^2} \quad \text{or} \quad d = \frac{a_0}{20} = 0.2236a_0$$

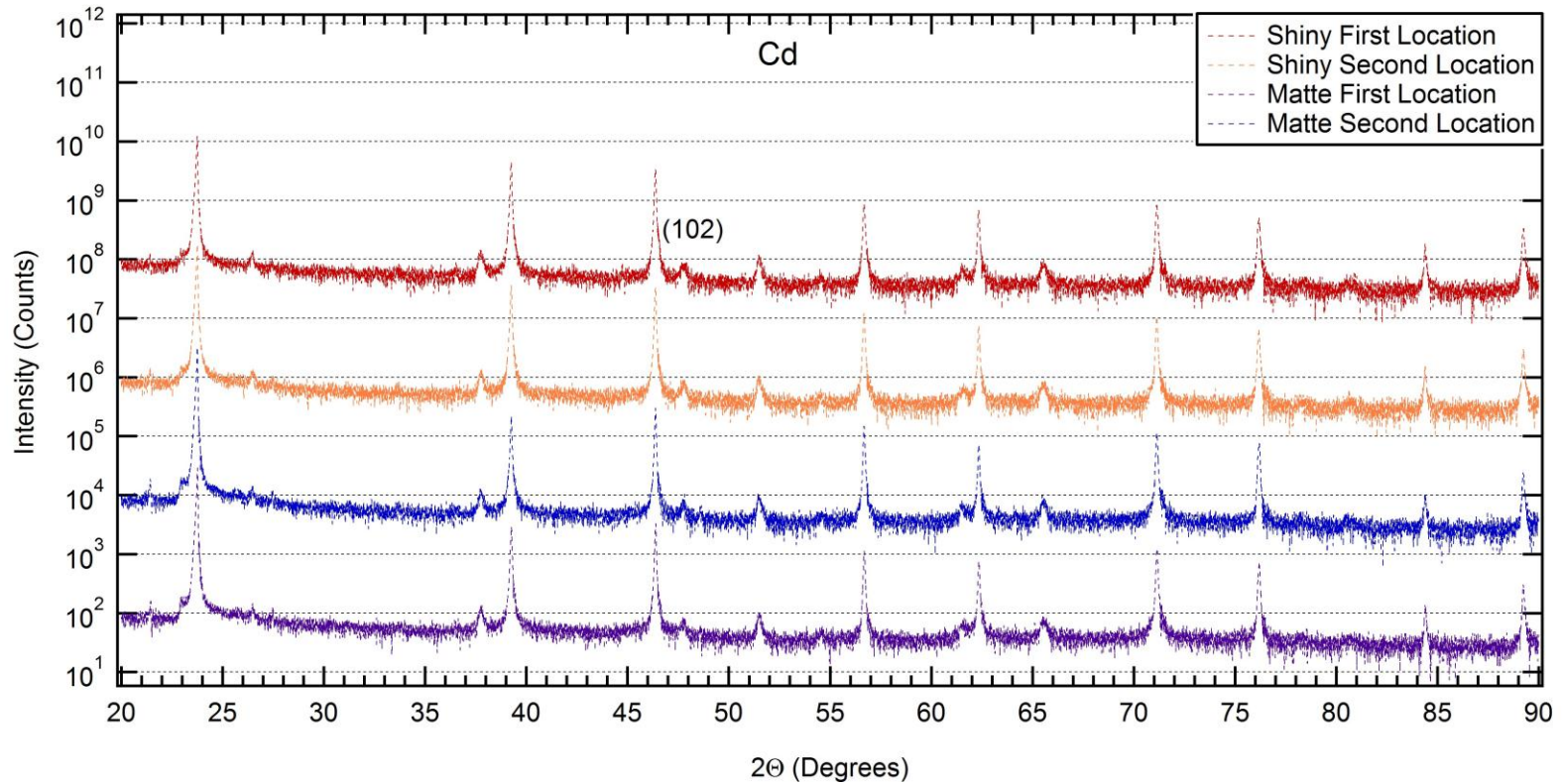
Not only can crystals be used to separate different x-ray wavelengths, but x-rays in turn can be used to study crystals, for example determine the type of crystal ordering and a_0 .

X-Ray diffraction (XRD) pattern (diffractogram) from NaCl



$$d_{hkl} = \frac{a_0}{\sqrt{h^2 + k^2 + l^2}}$$

Raw Data

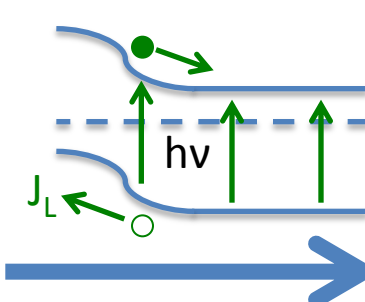
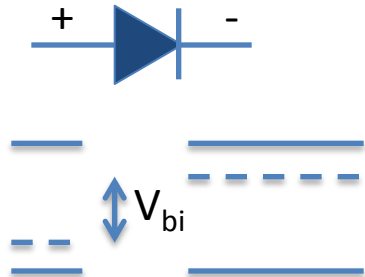


Peaks were considered if they were known CdTe peaks. Peaks from other layers (ex. CdS) were not included.

J-V and Spectra Response Characterization

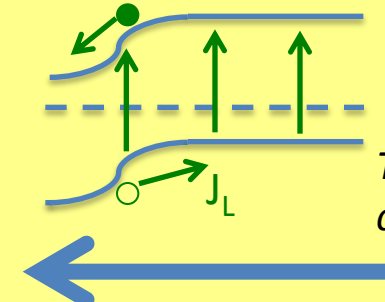
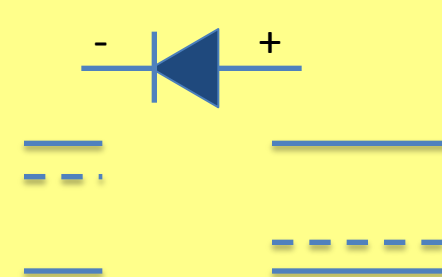
Homojunction solar cell (e.g., Silicon)

p-type emitter (window)
n-type base (absorber)



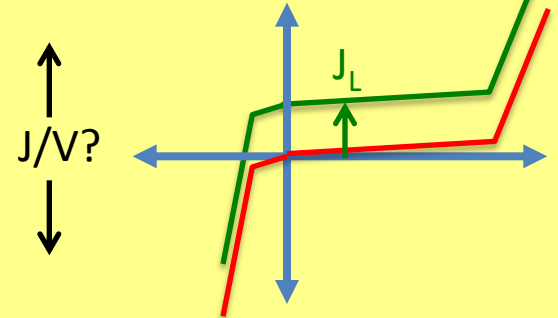
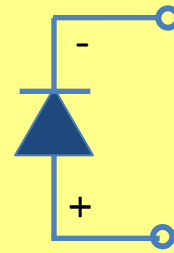
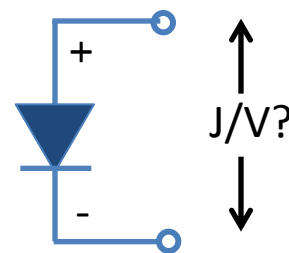
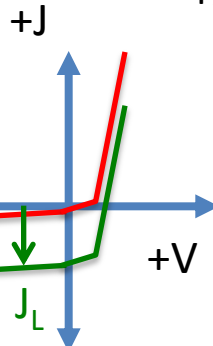
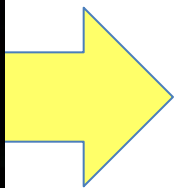
+J under forward bias

n-type emitter (window)
p-type base (absorber)



Typical Si device configuration

+J under forward bias



Light Generated Current is Opposite Direction of Forward Dark Current

Solar cell efficiency

The efficiency of a solar cell (sometimes known as the power conversion efficiency, or PCE, and also often abbreviated η) represents the ratio where the output electrical power at the maximum power point on the IV curve is divided by the incident light power – typically using a standard AM1.5G simulated solar spectrum.

The efficiency of a solar cell is determined as the fraction of incident power which is converted to electricity and is defined as:

$$P_{\max} = V_{OC} I_{SC} FF \qquad \eta = \frac{V_{OC} I_{SC} FF}{P_{inc}}$$

where V_{oc} is the open-circuit voltage;

where I_{sc} is the short-circuit current; and

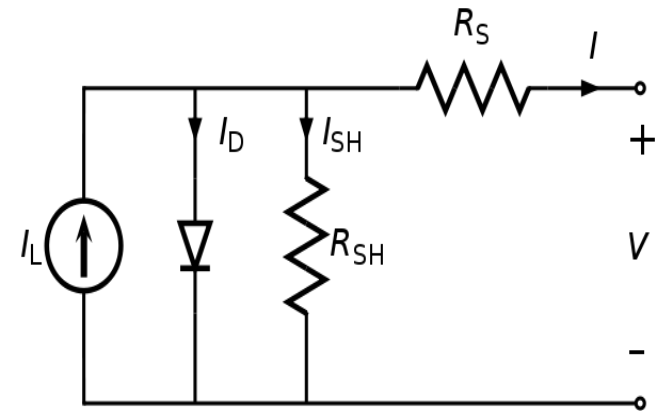
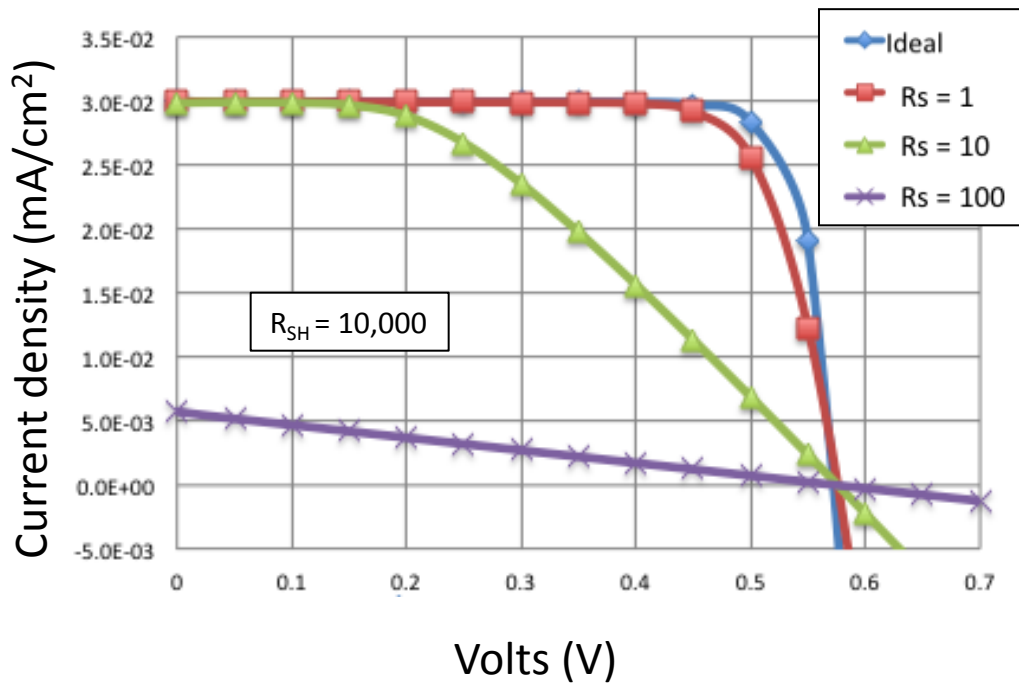
where FF is the fill factor

where η is the efficiency.

Power in AM1.5G spectrum is 1kW/m^2 , or 100 mW/cm^2

For a $10 \times 10\text{ cm}^2$ cell, the input power (AM1.5G) is $100\text{ mW/cm}^2 \times 100\text{ cm}^2 = 10\text{ W}$.

Impact of Electrical Loss Due to High Series Resistance (R_S) PV cells



Diode equation with R_S and R_{SH} :

$$I = I_L - I_0 \exp \left[\frac{q(V + IR_S)}{nkT} \right] - \frac{V + IR_S}{R_{SH}}$$

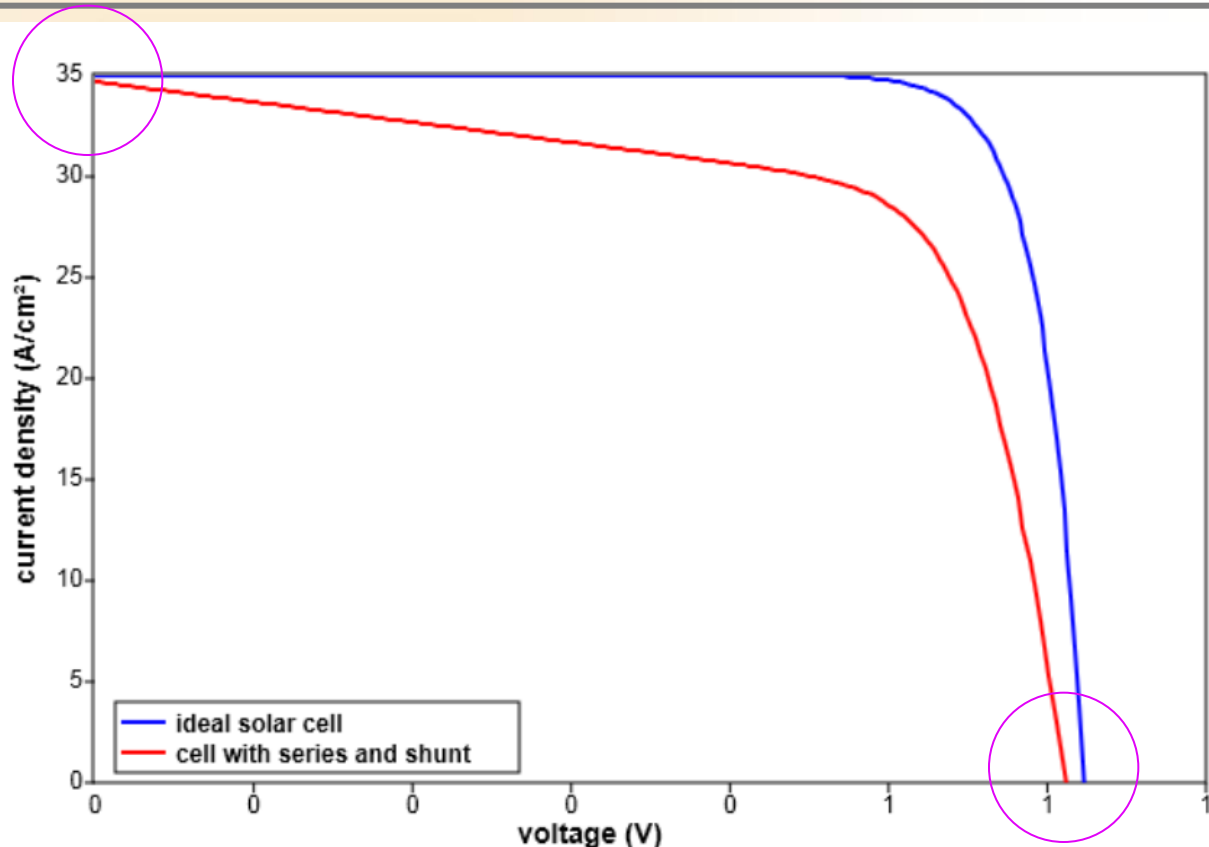
Solar cell series and shunt resistance

From <http://www.pveducation.org/pvcdrom/solar-cell-operation/series-resistance>

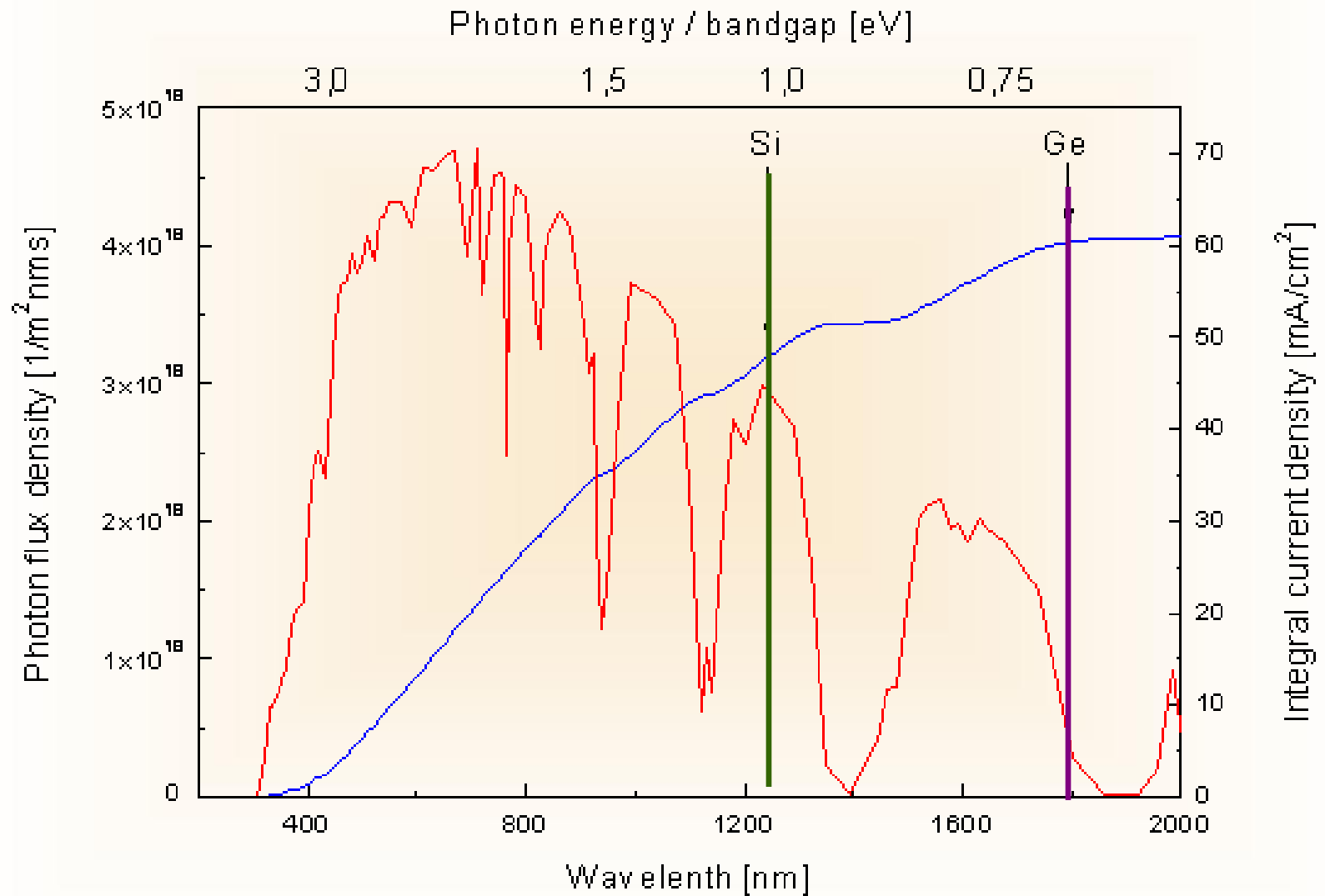
Series resistance (R_s) in a solar cell has three causes: (1) the movement of current through the front contact and the semiconductor absorber region of the solar cell; (2) contact resistance between the metal contact and the silicon; and (3) resistance of the top and rear metal contacts. A high series resistance reduces the fill factor, and excessively high values may also reduce the short-circuit current.

Significant power losses caused by the presence of a **shunt resistance** (R_{sh}) are typically due to manufacturing defects, rather than poor solar cell design. Low shunt resistance causes power losses in solar cells by providing an alternate current path for the light-generated current.

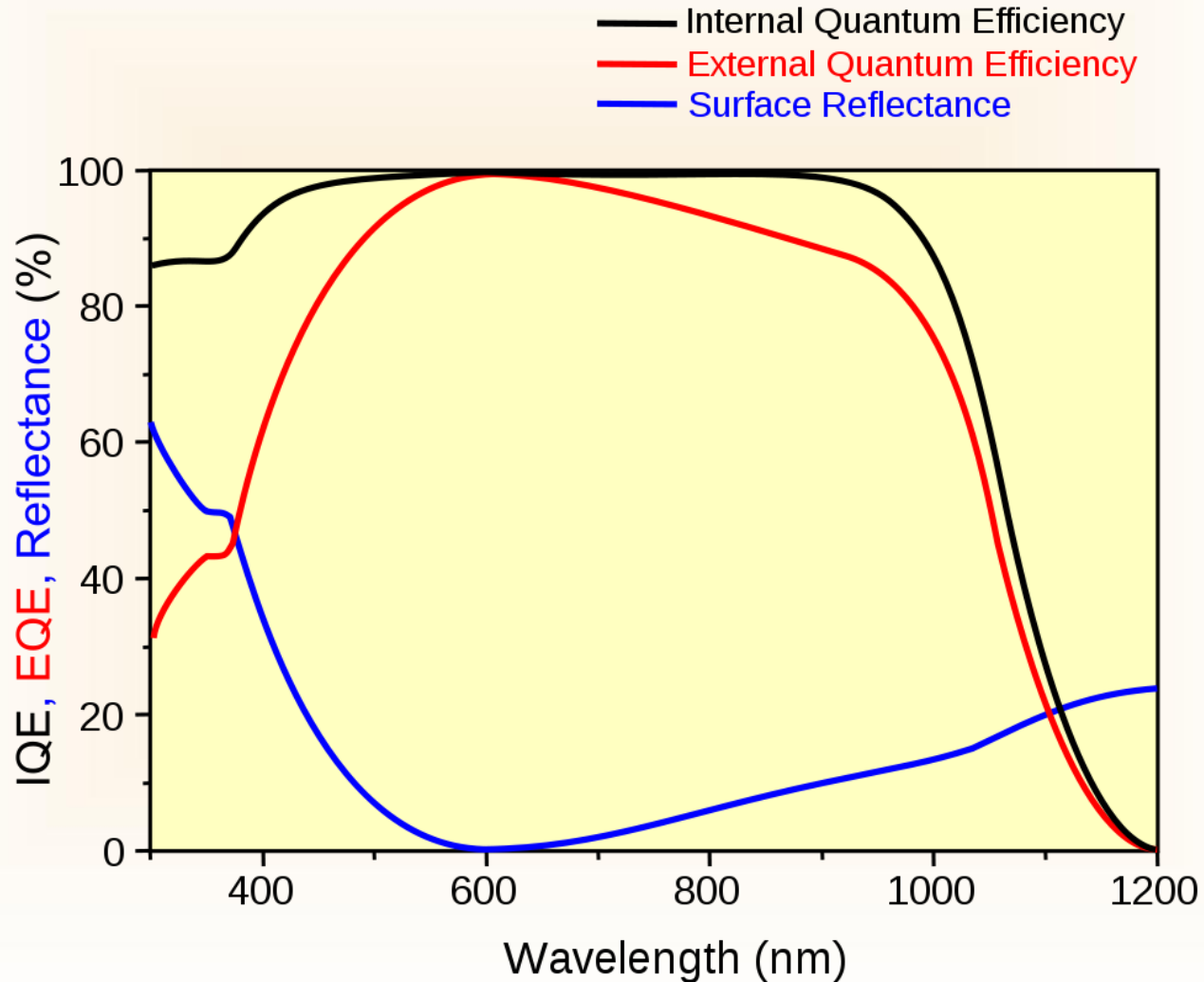
We have measured I vs. V , so that for I in Amps and V in Volts, the apparent resistance (Ω) at any point on the curve is given by: $(-1)/\text{slope}$. The shunt resistance is defined at $V = 0$ V, and the series resistance is defined at $V = V_{OC}$. For optimal power generation, solar cells should have a large R_{sh} and a small R_s .



Integrating the Solar Spectrum

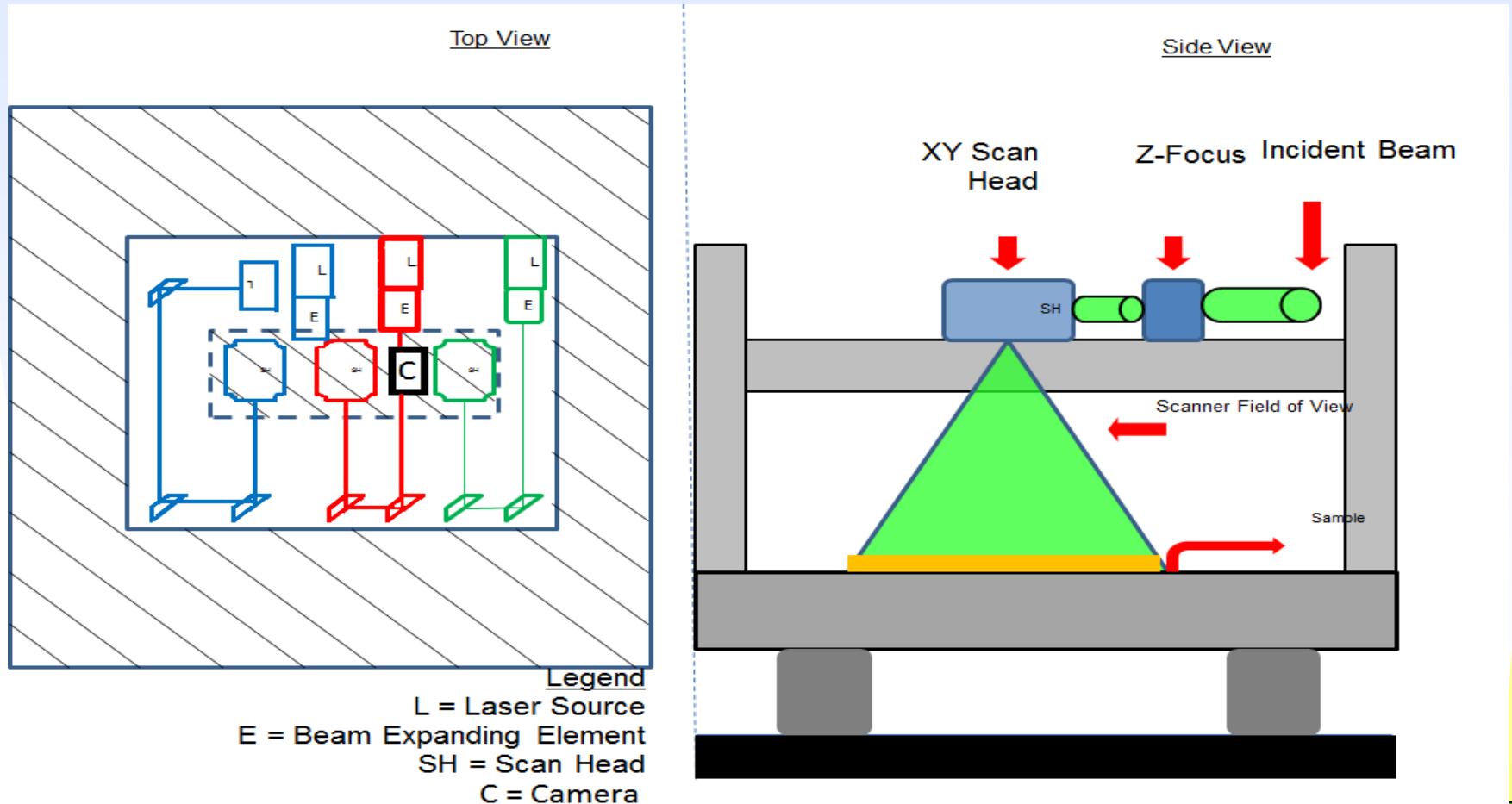


Spectral Response of a typical c-Si solar cell



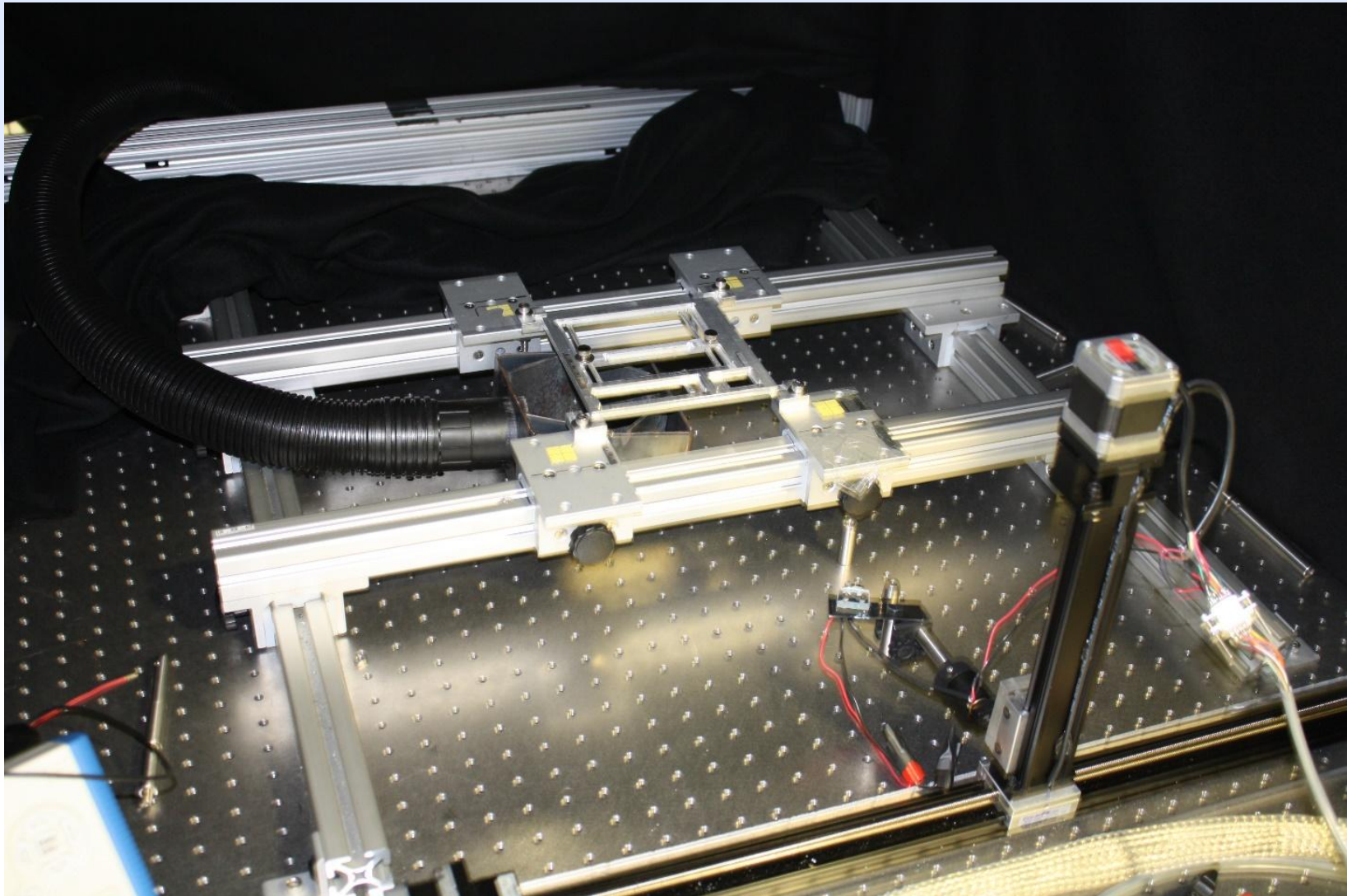
UT's Laser Scriber System

- 3 wavelengths (1064 nm, 532 nm, 355 nm) for addressing specific materials based on absorption spectrum.
- 60 cm x 60 cm flat field based on z-focus.



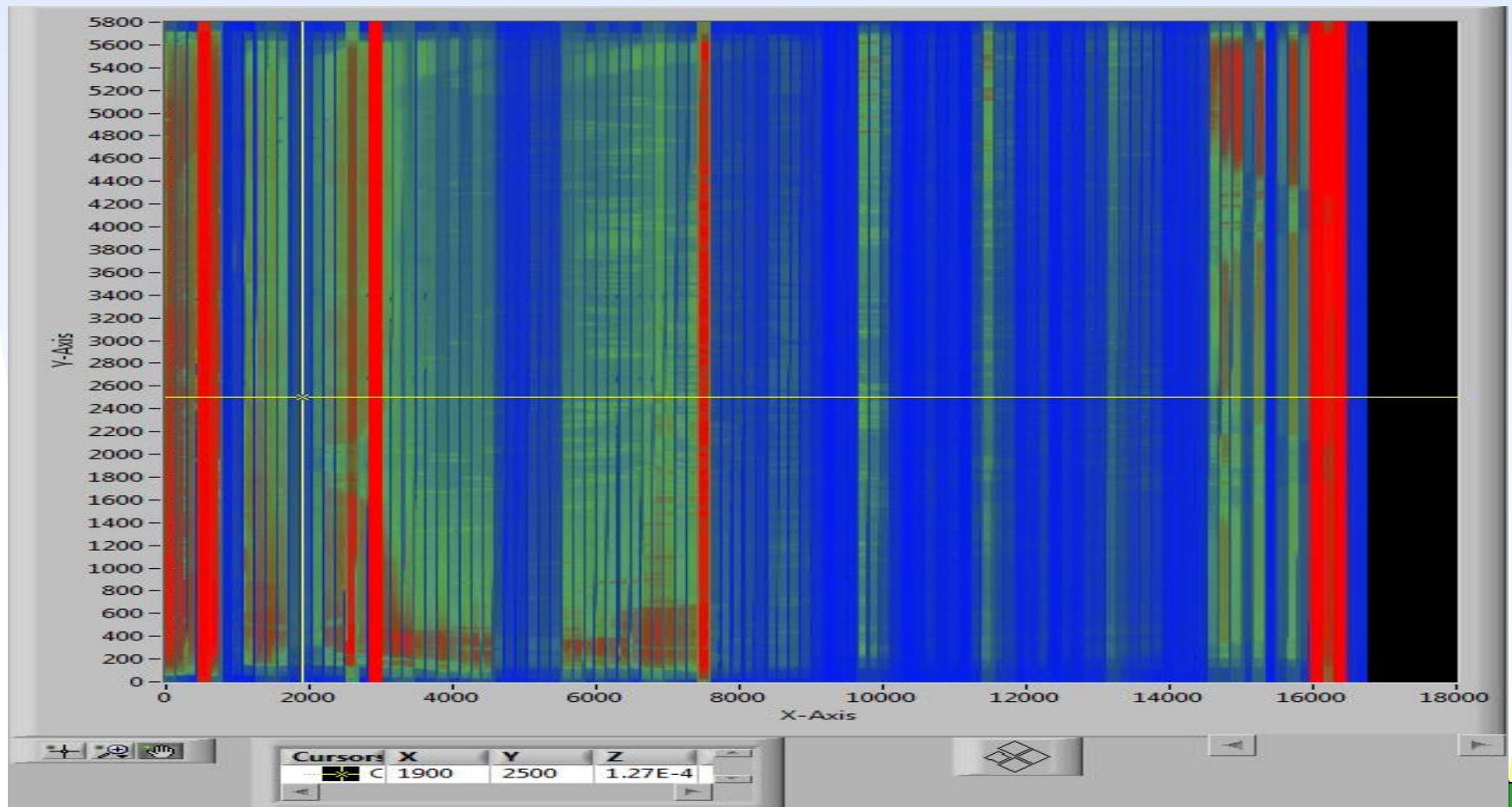
UT's Laser Scriber System

- Sample mounts; Motion control
- Exhaust handling (HEPA)



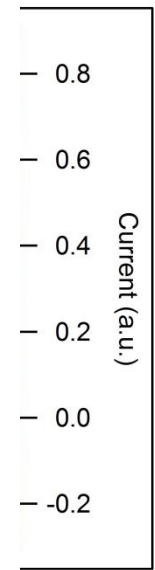
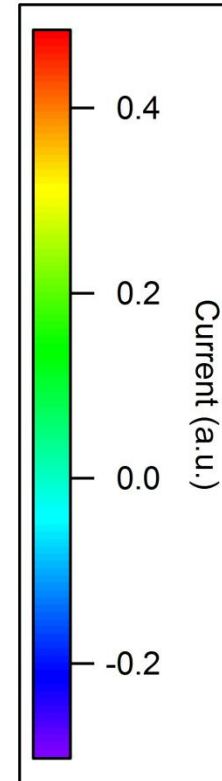
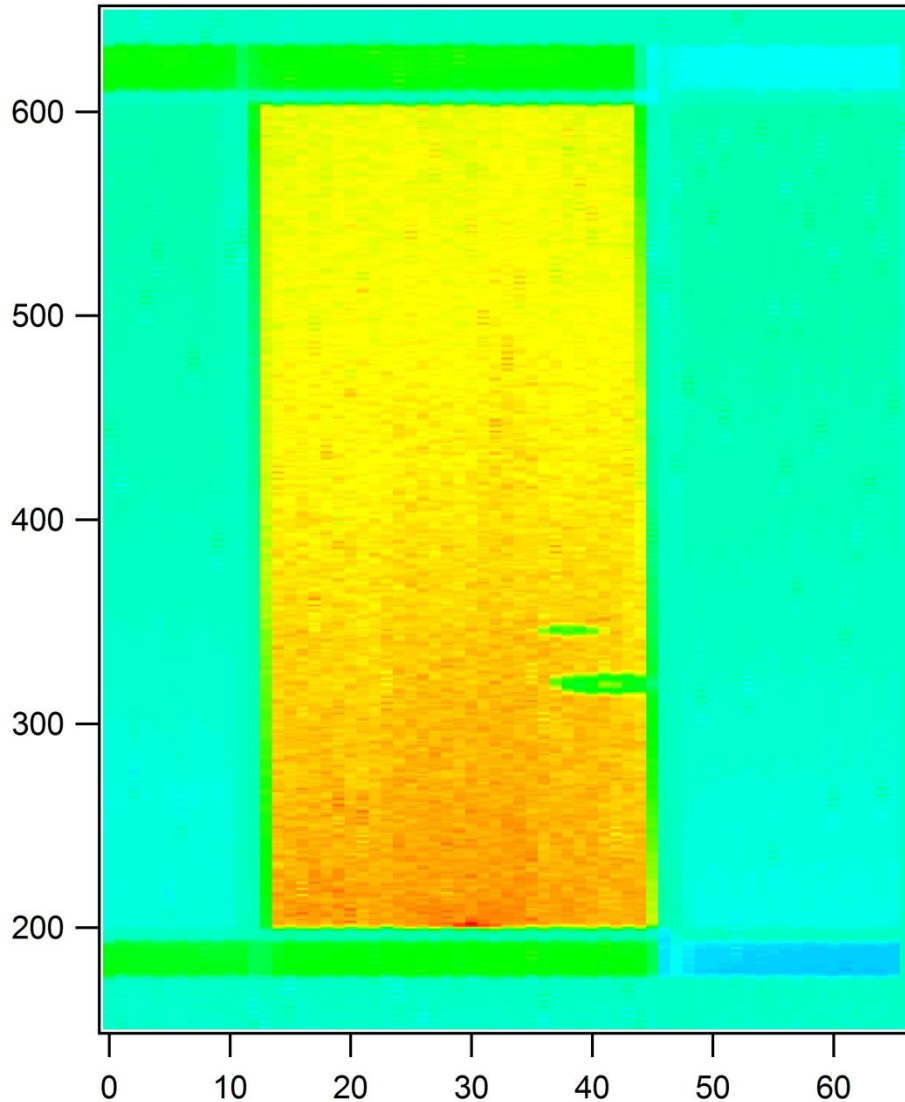
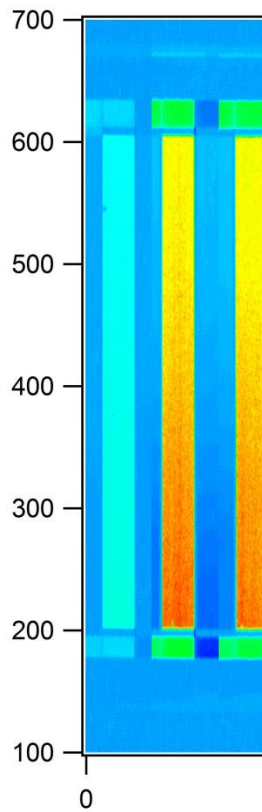
LBIC, LBIV

- Laser Beam Induced Current
- Laser beam induced Voltage
- Reveals cell layout for CdTe PV modules



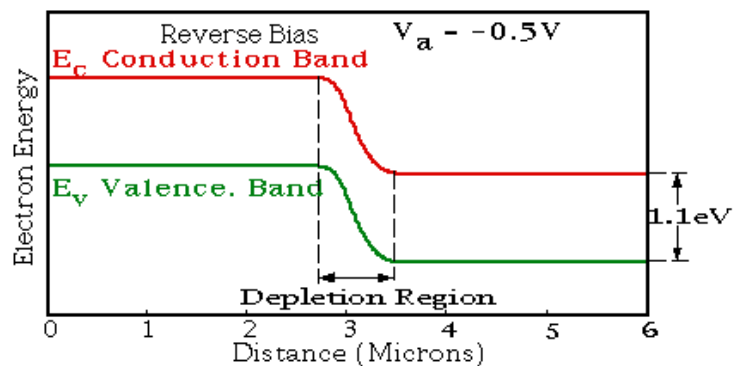
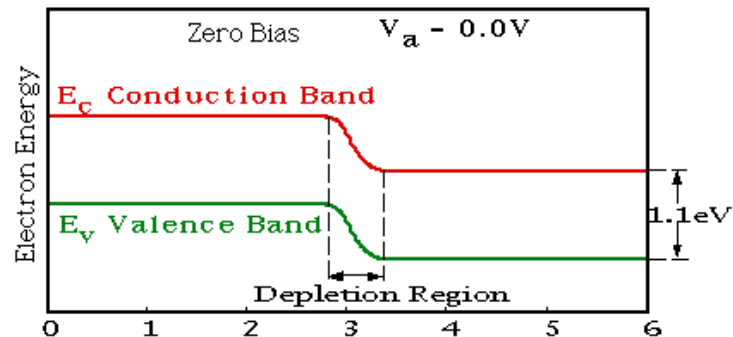
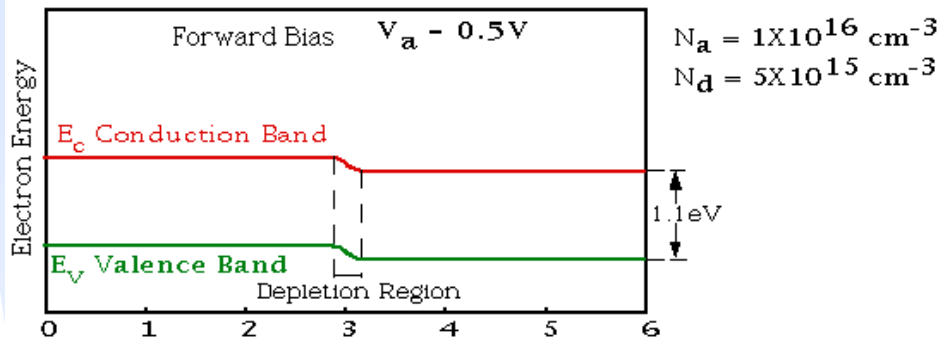
LBIC of CdTe mini-module

- CdTe mini-module, illuminated with 532 nm laser spot ($\sim 40 \mu\text{m}$ diameter)
- Later
- Scratch



Achieve charge separation

Energy Band Diagram for p-n diode



Achieve charge separation, directing electron and holes to different contacts (e.g., use doped materials for p-n junction)...

Prepare your materials and junctions to establish a built-in electric field. How?

Homojunction: (junction between two layers of the same material, which can differ by doping, structure, etc. but show the same dominant elemental makeup) -- must vary the chemical potential of the material (Fermi level) across the interface between n-type and p-type.

Achieve charge separation

Achieve charge separation, directing electron and holes to different contacts (e.g., use doped materials for p-n junction)...

Prepare your materials and junctions to establish a built-in electric field.
How?

Heterojunction: (junction between two different semiconductor materials) -- must create an energy band structure that promotes charge separation – a combination of energy band offsets and doping.

How do we measure the **dopant type and density**?

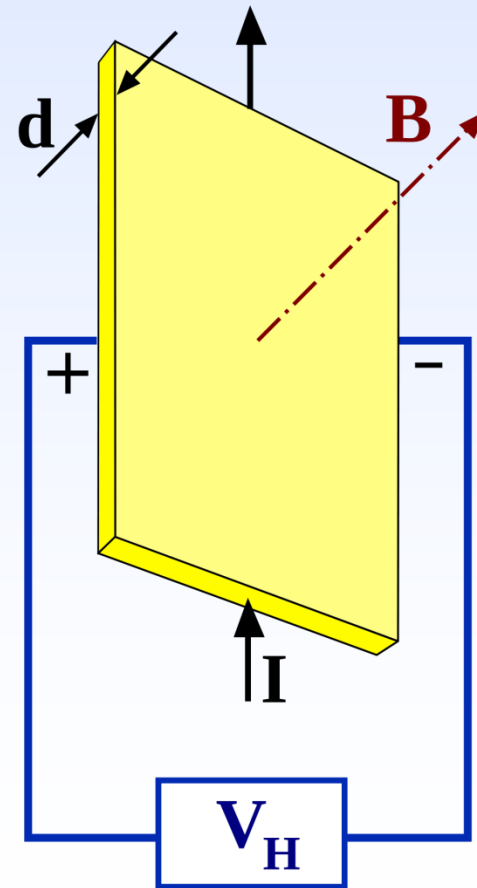


Measuring dopant type and density

Hall Effect: The Lorentz force, $F = -q\mathbf{v} \times \mathbf{B}$, deflects carriers to the left and right as they pass through a material under the influence of a magnetic field. The induced voltage lateral to the current flow direction provides information about the Hall coefficient, which can then be related to the carrier density and mobility:

$$R_H = \frac{E_y}{J_x B_z}$$

$$\mu = \frac{R_H}{\rho} \quad n = \frac{1}{eR_H}$$



Preston and Dietz, (Expt. 17; pp 303-315)

Measuring dopant type and density (Mott Schottky)

C_{sc} = capacitance of the space charge region

ϵ = dielectric constant of the semiconductor

ϵ_0 = permittivity of free space

N = donor density (electron donor concentration for an n -type semiconductor or hole acceptor concentration for a p -type semiconductor)

E = applied potential

E_{fb} = flatband potential

Mott-Schottky plots ($1/C^2$ vs. E)

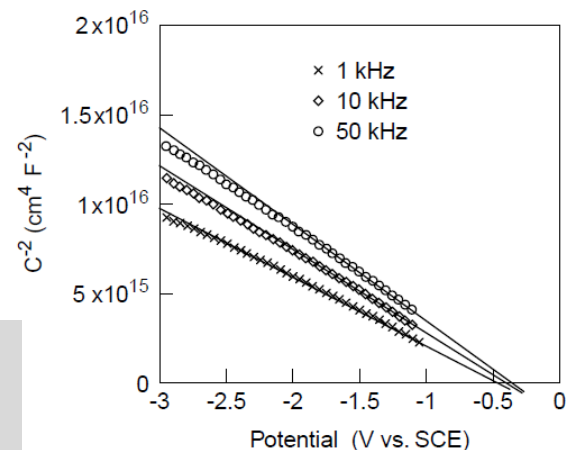
$$C = \frac{Q}{V} = \frac{\epsilon A}{W_d}$$

Mott-Schottky: measuring in depletion, not in accumulation. Changing the depletion width by applied voltage; when the capacitance reaches a maximum \rightarrow flat band potential.

$$W = \left[\frac{2K_s\epsilon_0}{q} \left(\frac{N_A + N_D}{N_A N_D} \right) (V_{bi} - V) \right]^{\frac{1}{2}}$$

F8

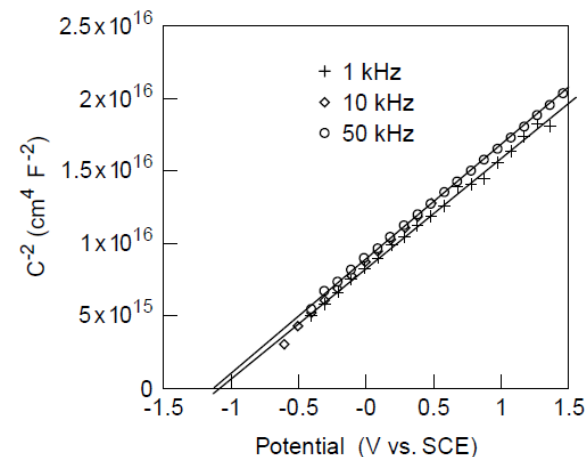
Mott-Schottky plot for a p -type semiconductor (figure adapted from ref. 2).



Sign of slope determined by free carrier type; slope related to free carrier density

F9

Mott-Schottky plot for an n -type semiconductor (figure adapted from ref. 2).



<http://www.currentseparations.com/issues/17-3/cs-17-3d.pdf>

Hot Probe Test to determine Carrier Type

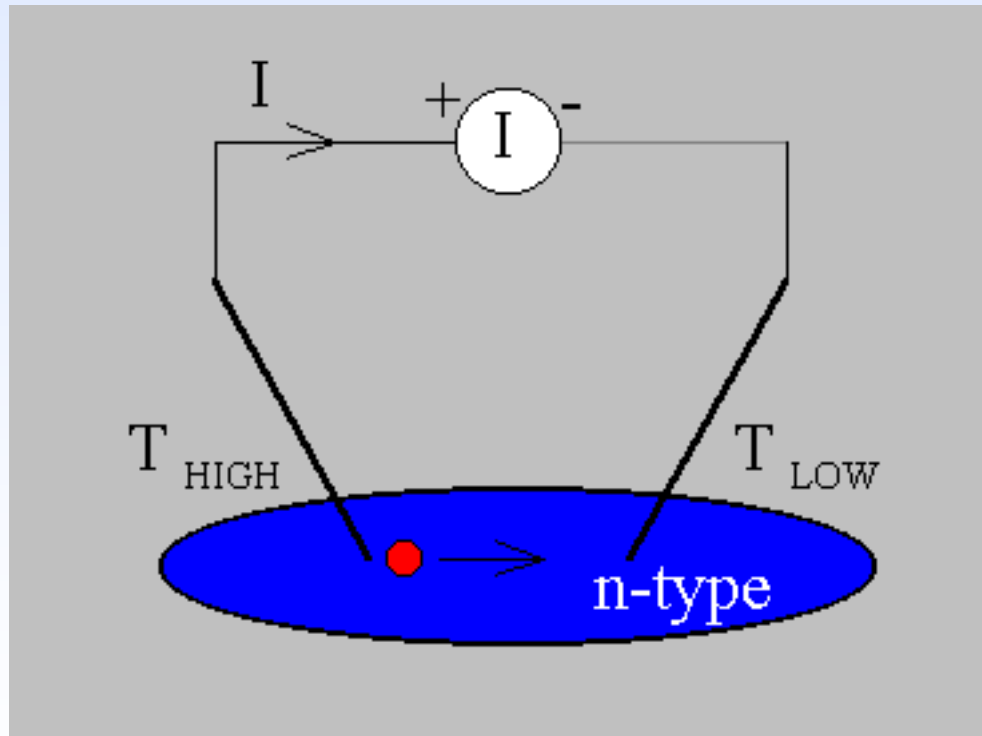
Seebeck Effect

- In 1821, Thomas Seebeck discovered that an electric current would flow continuously in a closed circuit made up of two dissimilar metals if the junctions of the metals were maintained at two different temperatures.
- When a metal wire is connected between two different temperatures, an additional number of electrons are excited at the hot end versus the cold end.
- Electrons drift from the hot end to the cold, and
- A thermal emf develops to oppose the drift
- If the material is uniform, the magnitude of the voltage developed depends only on the temperature difference.
- The Hot Probe is the trivial case.....i.e., no junctions.



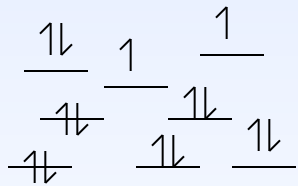
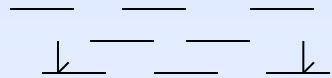
Hot Probe Test to determine Carrier Type

All you need is a soldering iron, and an ammeter!



Hot Probe Test to determine Carrier Type

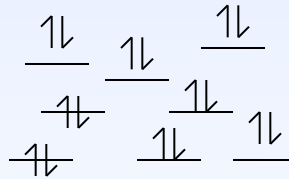
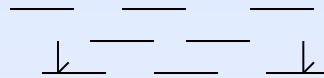
Intrinsic



$$p = n = n_i$$

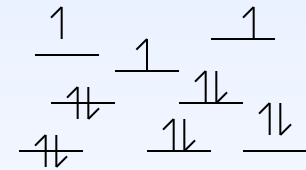
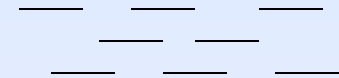
Number of thermally generated Holes equals number thermally generated free electrons

n-type



Number of free electrons equals number of positively charged donor ions

p-type



Number of free holes equals number of Negatively charged acceptor cores



Hot Probe Test to determine Carrier Type

Distribution of OCCUPIED C.B. levels:



Hot

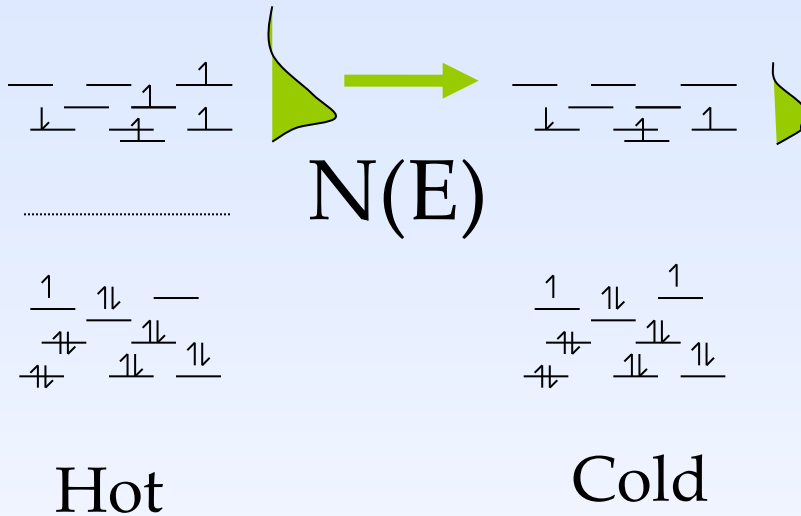
Cold

These are *not* in equilibrium!



Hot Probe Test to determine Carrier Type

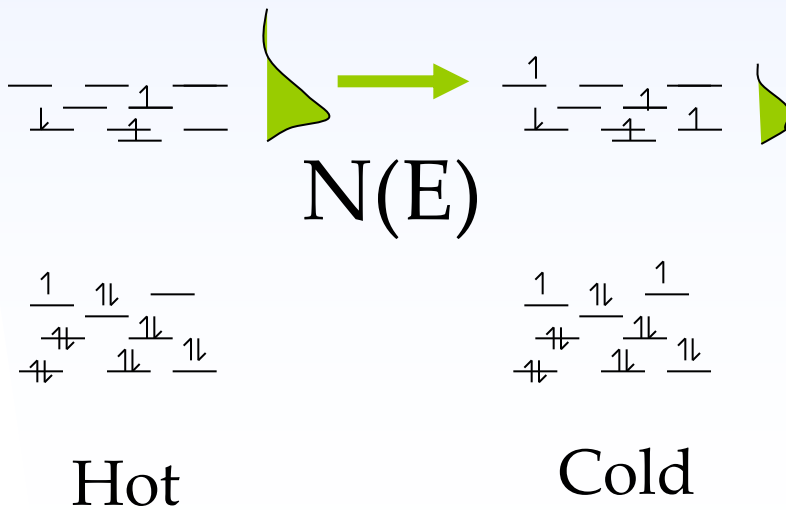
Seebeck effect, n-type semiconductor



Fick's Law of Diffusion:

$$J = -D \frac{\partial c}{\partial x}$$

Electrons diffuse from region of high Concentration to region of lower concentration



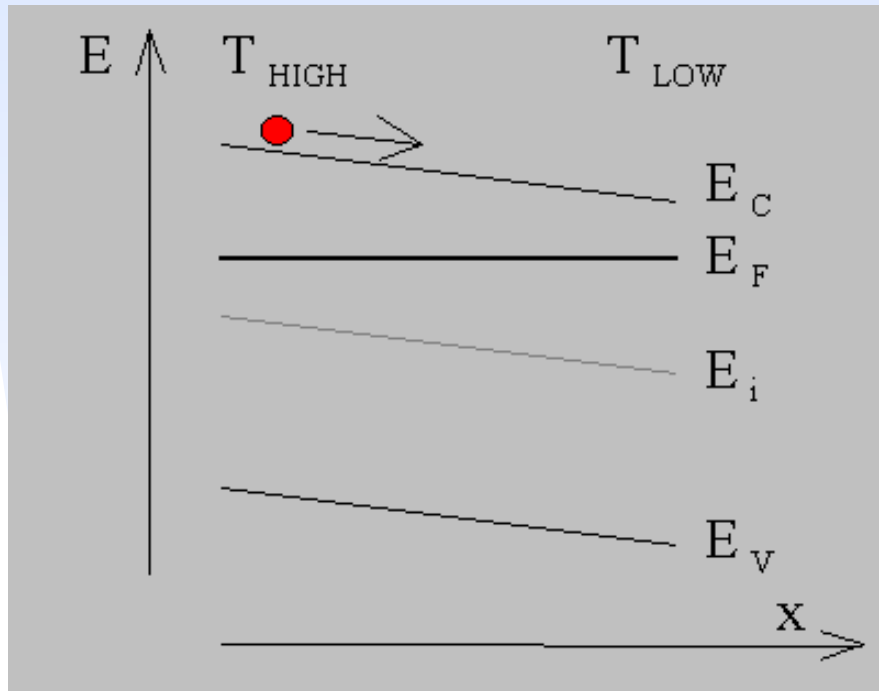
"Cold" side becomes slightly negatively charged
Hot side becomes positively charged

After Hamers



Hot Probe Test to determine Carrier Type

Another way to look at what is happening:



Fermi energy remains constant throughout the material. The variation in free carrier density then changes the positions of the CB and VB as a function of temperature (position).

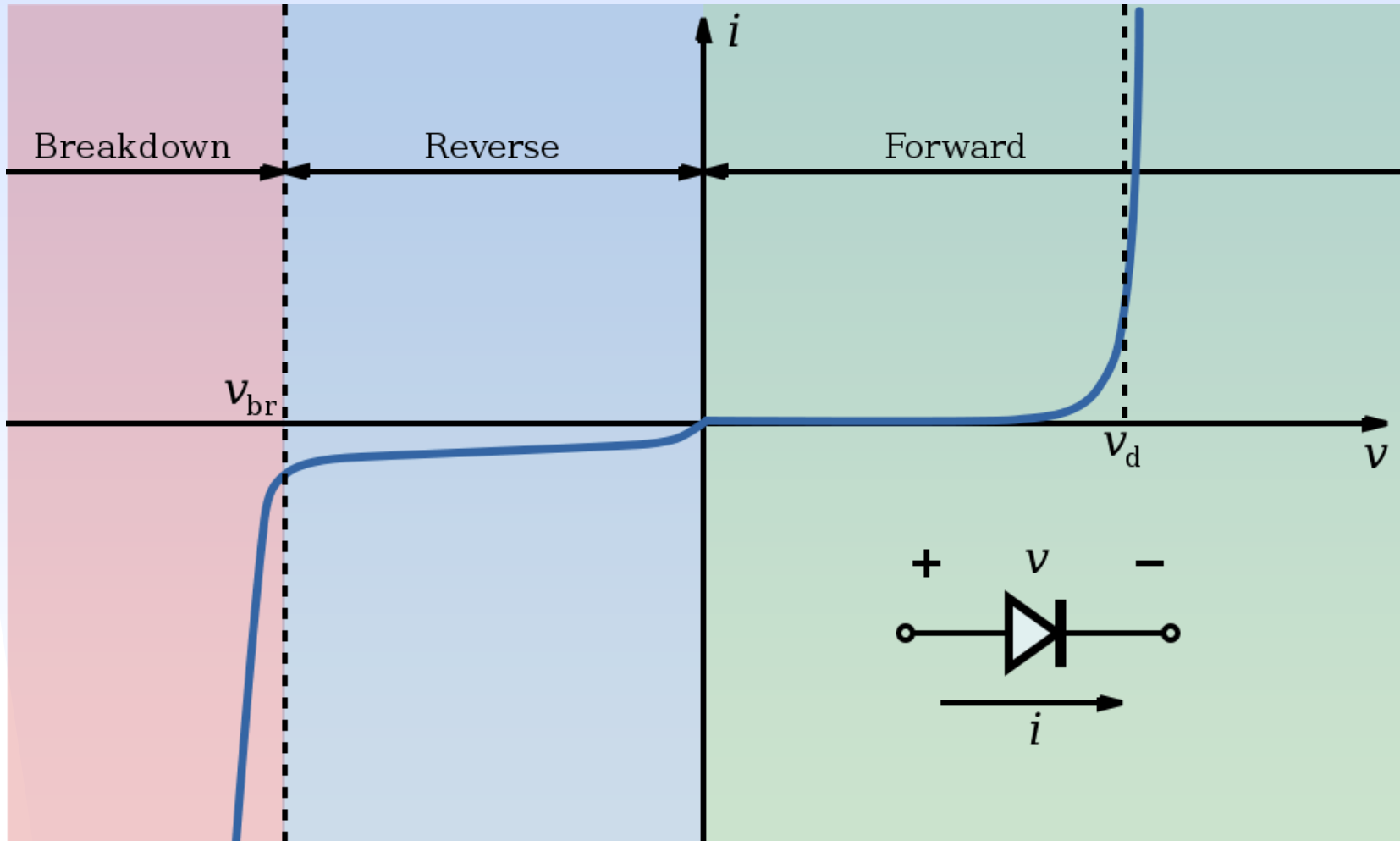
“As the effective density of states decreases with decreasing temperature, one finds that the conduction band energy decreases with decreasing temperature yielding an electric field which causes the electrons to flow from the high to the low temperature. The same reasoning reveals that holes in a p-type semiconductor will also flow from the higher to the lower temperature.”

$$J = \mu_n n \left(\frac{\partial E_F}{\partial x} - q\mathcal{P} \frac{\partial T}{\partial x} \right)$$

$$q\mathcal{P} = -k \left(\frac{5}{2} - \frac{T}{\mu_n} \frac{\partial \mu_n}{\partial T} + \ln \frac{N_C}{n} \right)$$



Rectifying behavior



I-V characteristics of a P-N junction diode (not to scale). From <http://en.wikipedia.org/wiki/Diode>